European Journal of Radiology 112 (2019) 44–51

Contents lists available at ScienceDirect

European Journal of Radiology

journal homepage: www.elsevier.com/locate/ejrad

Research article

Prediction of EGFR mutations by conventional CT-features in advanced pulmonary adenocarcinoma

Yanqing Chen[a,1], Yang Yang[b,1], Longbai Ma[a,1], Huiyuan Zhu[c], Tienan Feng[d], Sen Jiang[b], Youyong Wei[a], Tingting Wang[b], Xiwen Sun[b,*]

[a] Department of Radiology, People's Hospital of Guangxi Zhuang Autonomous Region, Nanning, China
[b] Department of Radiology,Shanghai Pulmonary Hospital,Tongji University School of Medicine,Shanghai, China
[c] Department of Nuclear Medicine, Shanghai Tenth People's Hospital Affiliated Tongji University, Shanghai, China
[d] Clinical Research institude, Shanghai Jiaotong University School of Medicine, Shanghai, China

ARTICLE INFO

Keywords:
Computed tomography (CT)
Epidermal growth factor receptor (EGFR) mutations
Advanced pulmonary adenocarcinoma

ABSTRACT

Objective: This study assessed the ability of conventional computed tomography (CT) features (including primary tumors, metastatic lesions, lymph nodes, and emphysema) to predict epidermal growth factor receptor (EGFR) mutations in advanced pulmonary adenocarcinoma.

Methods: Patients who were diagnosed with advanced pulmonary adenocarcinoma between January 2017 and August 2017 and had undergone a chest CT and EGFR mutation testing were enrolled in this retrospective study. Qualitative and quantitative CT-features and clinical characteristics evaluated in this study included: primary tumor location, size, and morphology (including degree of lobulation, density, calcification, cavitation, vacuole sign, and air bronchogram), size and distribution of lung and pleural metastatic nodules, size and status of hilar and mediastinal lymph nodes, emphysema, organs with distant metastasis, and patient age, sex, and smoking history.

Results: Of 201 patients, 107 (53.23%) were EGFR-mutation positive. The multivariate logistic regression indicated that EGFR mutations were significantly associated with smaller lymph nodes, a lower percentage of deep lobulation of the primary tumor and partial fusion of lymph nodes, and absence of emphysema. The area under the curve of logistic regression model for predicting EGFR mutations was 0.898.

Conclusions: Conventional CT-features, including emphysema, degree of primary tumor lobulation, and lymph node size and status, help to predict the presence or absence of EGFR mutations in advanced pulmonary adenocarcinoma. Additionally, these same CT-features demonstrated that the CT manifestations of the EGFR mutant group were of relatively lower malignancy and less invasive as compared to the wild-type EGFR group.

1. Introduction

Lung cancer is one of the leading causes of death worldwide. More than 85% of lung cancers are non-small cell lung cancer (NSCLC); adenocarcinoma is the most common subtype of NSCLC [1]. Due to the lack of early specific signs and symptoms, most lung cancer patients are diagnosed at advanced stages and thus are not eligible for curative surgery; hence, the prognosis for these patients is usually poor [2]. In the last decade, the advent of novel therapeutics that target genetically-altered signaling pathways has revolutionized treatment options for NSCLC patients [3]. Epidermal growth factor receptor tyrosine kinase inhibitor (EGFR TKI) targeted therapy has shown promising benefits for patients with advanced NSCLC. Mutations in the gene encoding EGFR are strong predictors of how well patients with advanced NSCLC will respond to EGFR TKIs [4,5].

CT-imaging plays an important role in diagnosing lung cancer and evaluating responses to treatment. Previous studies suggested that features of CT or CT-based radiomics may be associated with EGFR mutations [6–15]. To date, most studies of CT-features or CT-based radiomics of EGFR mutations focused on early-stage and resectable NSCLC or on all stages of NSCLC. However, the main patient population that received EGFR TKI targeted therapy had advanced NSCLC. Additionally, different stages of NSCLC contain different CT-features. Furthermore, these studies mainly focused on primary tumors; only a

* Corresponding author at: Department of Radiology,Shanghai Pulmonary Hospital,Tongji University School of Medicine,507 Zhengmin Road, Shanghai,200433, China.
E-mail address: sh2010gx2013@163.com (X. Sun).
[1] These authors contributed equally to this work.

https://doi.org/10.1016/j.ejrad.2019.01.005
Received 4 August 2018; Received in revised form 10 December 2018; Accepted 5 January 2019
0720-048X/ © 2019 Elsevier B.V. All rights reserved.

few of them studied metastatic lesions or lymph nodes. However, development of lung cancer targeted therapies and validation of therapeutic response biomarkers will require analysis of both primary and metastatic cancers, based on evidence of intra-tumor genetic heterogeneity and genetic heterogeneity between primary and metastatic tumors in lung cancers [16,17].

To the best of our knowledge, previous studies of advanced pulmonary adenocarcinoma have not assessed the value of conventional CT-features (including evaluation of primary tumors, metastatic lesions, lymph nodes, and emphysema) in predicting EGFR mutations. Therefore, the purpose of this study was to assess the value of using conventional CT-features to predict the presence of EGFR mutations in advanced pulmonary adenocarcinoma.

2. Materials and methods

2.1. Ethical approval

This study was approved by the Institutional Review Board of Shanghai Pulmonary Hospital as a retrospective study; thus, the requirement for patient informed consent was waived.

2.2. Patient selection

Patients with unresectable, advanced pulmonary adenocarcinoma who were diagnosed between January 2017 and August 2017 and had undergone a chest CT and EGFR mutation testing at Shanghai Pulmonary Hospital were enrolled in this study. Staging was conducted according to the staging system of the International Association for the Study of Lung Cancer (version 8). All patients had no prior diagnosis of lung cancer and had not been treated for lung cancer. Patients samples were excluded from the study based on the following criteria: inadequate for EGFR mutation testing, > 1 month between CT imaging and the EGFR mutation testing.

For each patient, the date of CT examination, cancer stage, presence of distant metastases, sex, age, and smoking status (current smoker or former smoking within previous 10 years) were extracted from medical records.

2.3. Mutation detection

Tumor specimens were obtained via bronchoscopic biopsy or CT-guided core biopsy before the initiation of therapy. EGFR mutations were detected using commercially available kits from Amoy Diagnostics (Xiamen, China). These kits are based on amplification refractory mutation system (ARMS) real-time polymerase chain reaction (PCR) technology. These kits can detect mutations in exons 18–21, including G719X in exon 18, 19-del in exon 19, T790 M, S768I, and 20-ins in exon 20, and L858R and L861Q in exon 21. All tests were performed according to the manufacturer's protocol.

2.4. CT image acquisition

CT examinations were randomly performed on a 128-detector row Brilliance iCT (Royal Philips, Netherlands), a 64-detector row SOMATOM Definition AS + (Siemens Healthineers, Germany), or a 64-detector row United Imaging uCT760 (United Imaging, China), with the following parameters: collimation: 38.4 mm (64 × 0.6 mm) to 80 mm (128 × 0.625 mm), beam pitch: 0.804–1.2, tube rotation time: 0.5 s, tube voltage: 120 kVp, tube current: 100–450 mA, slice thickness: 0.6 mm or 0.625 mm, reconstruction thickness: 1.0 mm, and reconstruction intervals: 0.7 mm or 1.0 mm. Each CT image encompassed the lower neck to the level of the adrenal glands; 72.41% of patients were examined by CT after enhancement with an intravenous contrast medium.

2.5. Evaluation of CT features

Two radiologists with 7 years and 26 years of experience independently interpreted the CT images of the target lesions. Both radiologists were aware that the CT images corresponded to lung adenocarcinoma patients but were unaware of the EGFR mutation status. Interpretation of CT images was done on a mediastinal window (M, 40; W, 400) and lung window (M, −450; W, 1500) using a picture archiving and communication system. The images were analyzed for the following points: 1) site of the tumor, indicated as right upper lobe (RUL), middle lobe (ML), right lower lobe (RLL), left upper lobe (LUL), left lower lobe (LLL), or mixed when the tumor had infiltrated more than one lobe, 2) location of the tumor described as central, peripheral, or mixed when present in both central and peripheral parts, 3) tumor size, noted as measurable or unmeasurable (i.e., the margin of the tumor was obscured and unclear because of complications with atelectasis); for measurable tumors, tumor size values corresponded to the mean of the longest and shortest diameters on the largest axial surface of the primary tumor; 4) tumor density, described as ground glass opacity (GGO), mixed GGO, or solid; 5) presence or absence of calcifications; 6) presence or absence of cavitation; 7) presence or absence of vacuole sign; 8) presence or absence of air bronchogram; 9) lobulation, described as shallow lobulation, deep lobulation (i.e., lobulation with chord distance/chord length > 0.4 and chord distance/tumor size > 0.4) (Fig. 1A–D), no lobulation, or obscured (i.e., tumor complicated with pulmonary atelectasis); 10) distribution of pulmonary metastatic nodules, indicated as ipsilateral lung (i.e., nodules in primary tumor lung), contralateral lung (i.e., nodules in non-tumor lung), bilateral lung, or none; 11) distribution of pleural metastatic nodules, indicated as ipsilateral pleura, contralateral pleura, bilateral pleura, or none; 12) presence or absence of pulmonary and/or pleural metastatic nodules; 13) pulmonary and pleural metastatic nodule size, indicated as the mean value of the longest and shortest diameters on the largest axial surface of the largest nodules; 14) presence or absence of swollen lymph nodes in the hilar and mediastinum; 15) hilar and mediastinal lymph node size; 16) hilar and mediastinal lymph node status, indicated as solitary lymph nodes, partial fusion of lymph nodes, extensive fusion of lymph nodes (fused lymph nodes/total lymph nodes > 2/3) (Fig. 1E–P), or none (no swollen lymph nodes); and 17) presence or absence of emphysema. If the examiners' interpretations were different, a joint session was held to reach a final decision by consensus.

2.6. Statistical analysis

CT features and clinical characteristics were expressed as mean ± standard deviation (SD) for continuous variables and as frequency and percentage for categorical variables.

The inter-observer agreement for qualitative CT-features was assessed by k statistics. The k value was ranked as follows: 0.00-0.20: poor; 0.21-0.40: fair; 0.41-0.60: moderate; 0.61-0.80: good; and 0.81–1.00: excellent.

Univariate analysis was performed to assess the association of clinical characteristics and CT features with EGFR mutations, using the Mann-Whitney U test for continuous variables and the chi-square test for categorical variables. Subsequent multivariate analysis was performed and odds ratios (OR) with 95% confidence intervals (CI) were calculated by a multivariate logistic regression model with stepwise selection of variables. The receiver operating characteristic (ROC) curve was constructed for the prediction of EGFR mutations according to each significant feature and with the full model, and the corresponding area under the curve (AUC) was calculated. P-values < 0.05 were considered significant. Bonferroni test corrected results of post-hoc comparison of single groups. A retrospective power analysis was conducted in the procedure of logistic regression. All statistical analyses were performed with the SPSS 17.0 software package (SPSS Inc., Chicago, IL, United States) or PASS 11.0 software (PASS 11. NCSS, LLC. Kaysville,

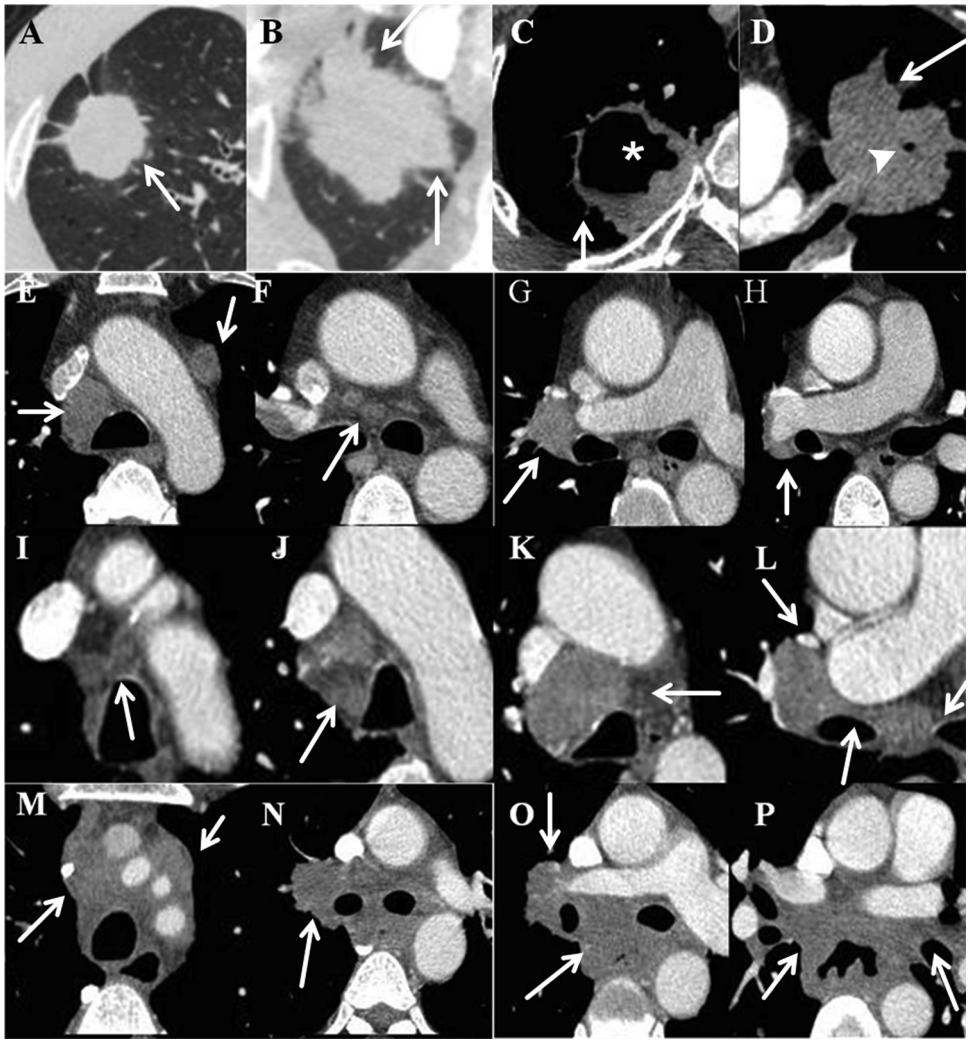

Fig. 1. CT features in advanced pulmonary adenocarcinoma patients. (A) shallow lobulation (arrow), (B) deep lobulation (arrows), (C) shallow lobulation (arrow) and cavitation (*), (D) deep lobulation (arrow) and vacuole sign (arrowhead), (E–H) status of solitary lymph nodes (arrows) at different CT levels in the same patient, (I–L) status of partial fusion of lymph nodes (arrows) at different CT levels in the same patient, and (M–P) status of extensive fusion of lymph nodes (arrows) at different CT levels in the same patient.

Utah, USA).

3. Results

3.1. Clinical characteristics of the study population

Clinical characteristics of the patient population are shown in Table 1. After applying inclusion and exclusion criteria, 201 patients were included in the study (mean age 63.00 ± 9.35 years; M:F = 117:84). EGFR mutations were detected in 107 of 201 patients (53.23%). The percentage of smokers in the patient population was 38.31%.

3.2. Interobserver agreement of CT interpretations

The concordance between the two observers was excellent, with k coefficients ranging between 0.810 and 0.976.

3.3. Relevance of clinical characteristics, CT features, and EGFR mutations

Based on univariate analysis, a significantly larger percentage of EGFR + patients were female ($P < 0.001$), non-smokers ($P < 0.001$), and did not have emphysema ($P < 0.001$) (Table 2). Additionally,

Table 1
Clinical Characteristics of the Study Population (N = 201).

	N/Total (%)
Age (years)[a]	63.00 (± 9.35)
Sex	
Male	117/201 (58.21)
Female	84/201 (41.79)
Smoking history	
Yes	77/201 (38.31)
No	124/201 (61.69)
Stage	
IIIB	36/201 (17.91)
IIIC	9/201 (4.48)
IV	156/201 (77.61)
Mutation type	
EGFR	107/201 (53.23)
EGFR wild-type	94/201 (46.77)
Distant metastases	
Boneb[b]	68/200 (34.00)
Brain[c]	25/200 (12.50)
Adrenals	6/201 (2.99)
Liver	10/201 (4.98)

[a] Mean (± SD).
[b] Bone metastasis was not assessed in 1 patient.
[c] Brain metastasis was not assessed in 1 patient.

Table 2
Relevance of Clinical Characteristics, CT Features, and EGFR Mutations (N = 201).

	EGFR			
	+N/Total (%)	−N/Total (%)	Univariate p-value	Multivariate Odds Ratio[b] (95%CI)
Age (years)[a]	62.21 (± 9.65)	63.88 (± 8.96)	0.185	
Sex			**< 0.001**	
Male	48/107 (44.86)	69/94 (73.40)		
Female	59/107 (55.14)	25/94 (26.60)		
Smoking	24/107 (22.43)	53/94 (56.38)	**< 0.001**	
Stage			**0.018**	
IIIB	14/107 (13.08)	22/94 (23.40)		
IIIC	2/107 (1.87)	7/94 (7.45)		
IV	91/107 (85.05)	65/94 (69.15)		
Lobe			0.170	
RUL	67/107 (62.62)	46/94 (48.94)		
ML	0	0		
RLL	1/107 (0.93)	2/94 (2.13)		
R mixed	1/107 (0.93)	1/94 (1.06)		
LUL	36/107 (33.64)	45/94 (47.87)		
LLL	0	0		
L mixed	2/107 (1.87)	0		
Tumor location[e]			**0.033**	
Central	5/107 (4.67)	14/94 (14.89)	**0.013**	
Peripheral	72/107 (67.29)	61/94 (64.89)	0.72	
Mixed	30/107 (28.04)	19/94 (20.21)	0.197	
Tumor size (cm)[a]	3.30 (± 1.30)	3.89 (± 1.64)	**0.011**	
Measurable	99/107 (92.52)	80/94 (85.11)		
Unmeasurable	8/107 (7.48)	14/94 (14.89)		
Tumor density			0.051	
Solid	98/107 (91.59)	92/94 (97.87)		
Mixed GGO	9/107 (8.41)	2/94 (2.13)		
Calcifications	7/107 (6.54)	5/94 (5.32)	0.715	
Cavitation	4/107 (3.74)	3/94 (3.19)	> 0.999	
Vacuole sign	6/107 (5.61)	7/94 (7.45)	0.597	
Air bronchogram	14/107 (13.08)	5/94 (5.32)	0.06	
Lobulation[e]			**< 0.001**	
Deep	32/107 (29.91)	60/94 (63.83)	**< 0.001**	**0.056 (0.013–0.233)**
Shallow	67/107 (62.62)	20/94 (21.28)	**< 0.001**	1.00 (Reference)
Obscured	8/107 (7.48)	13/94 (13.83)	0.142	
None	0	1/94 (1.06)		
Distribution of pulmonary metastatic nodules			0.215	
Ipsilateral	6/107 (5.61)	7/94 (7.45)		
Contralateral	13/107 (12.15)	8/94 (8.51)		
Bilateral	38/107 (35.51)	23/94 (24.47)		
None	50/107 (46.73)	56/94 (59.57)		
Distribution of pleural metastatic nodules			0.133	
Ipsilateral	40/107 (37.38)	23/94 (24.47)		
Contralateral	0	0		
Bilateral	7/107 (6.54)	6/94 (6.38)		
None	60/107 (56.07)	65/94 (69.15)		
Pulmonary and/or pleural metastatic nodules			**0.006**	
Yes	79/107 (73.83)	52/94 (55.32)		
No	28/107 (26.17)	42/94 (44.68)		
Pulmonary and pleural metastatic nodule size (cm)[a]	0.96 (± 0.63)	1.22 (± 0.76)	**0.021**	
Swollen lymph nodes			0.628	
Yes	101/107 (94.39)	91/94 (96.81)		
No	6/107 (5.61)	3/94 (3.19)		
Lymph node size (cm)[a]	1.74 (± 0.86)	2.55 (± 1.15)	**< 0.001**	**0.272 (0.099–0.748)**
Lymph node status[e]			**0.003**	
Extensive fusion	7/107 (6.54)	5/94 (5.32)	0.715	1.00 (Reference)
Partial fusion	13/107 (12.15)	32/94 (34.04)	**< 0.001**	**0.031 (0.002–0.522)**
Solitary	81/107 (75.70)	54/94 (57.45)	**0.006**	
None	6/107 (5.61)	3/94 (3.19)	0.628	
Emphysema	15/107 (14.02)	50/94 (53.19)	**< 0.001**	**24.338 (4.955–119.548)**
Bone metastasis	39/107 (36.45)	29/93 (31.18)[c]	0.433	
Brain metastasis	16/106 (15.09)[d]	9/94 (9.57)	0.239	
Adrenals metastasis	2/107 (1.87)	4/94 (4.26)	0.564	
Liver metastasis	6/107 (5.61)	4/94 (4.26)	0.909	

Note: significant ORs and p-values are in bold.

[a] Mean (± SD).

[b] Obtained by multiple logistic regression model with stepwise selection of variables.

[c] One patient was not evaluated for bone metastasis.

[d] One patient was not evaluated for brain metastasis.

[e] Regarding the univariate analysis, the Bonferroni correction alpha for tumor location, lobulation, and lymph node status is 0.0167, 0.0083, and 0.0083, respectively.

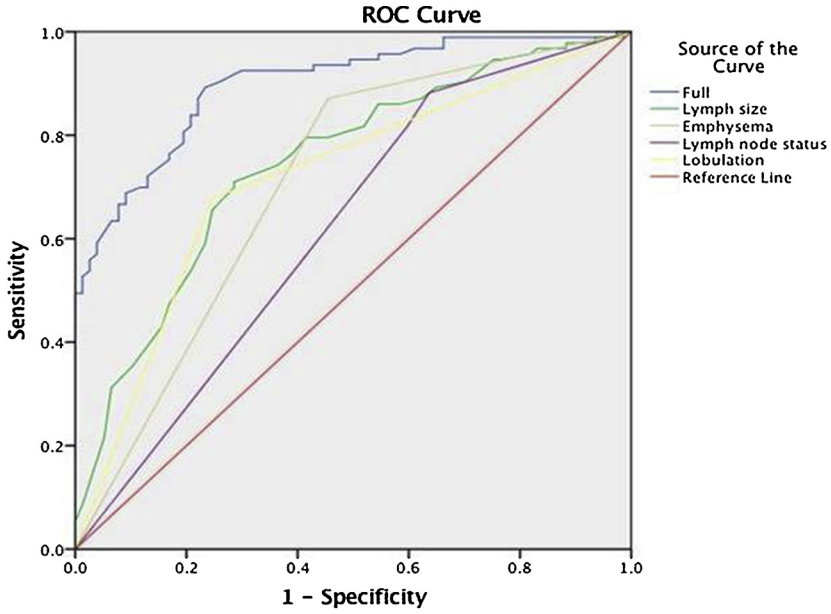

Area Under the Curve

Test Result Variable(s)	Area
Full	.898
Lymph size	.744
Emphysema	.708
Lymph node status	.619
Lobulation	.715

Fig. 2. Comparison between receiver operating characteristic curves for EGFR mutation prediction according to each significant feature and with the full model.

EGFR + patients had smaller primary tumors (P = 0.011), pulmonary and pleural metastatic nodules (P = 0.021), and lymph nodes (P < 0.001) (Table 2). A higher percentage of EGFR + patients had pulmonary and/or pleural metastatic nodules (P = 0.006), solitary lymph nodes (P = 0.006), and shallow lobulation of primary tumors (P = < 0.001); whereas a lower percentage of EGFR + patients had centrally located primary tumors (P = 0.013), deep lobulation of primary tumors (P < 0.001), and partial fusion of lymph nodes (P < 0.001) (Table 2). Subsequent multivariate analysis confirmed the significance of the following CT-features: absence of emphysema (OR, 24.338; 95%CI, 4.955–119.548), deep lobulation of primary tumors (OR, 0.056; 95%CI, 0.013-0.233), lymph node size (OR, 0.272; 95%CI, 0.099-0.748), and partial fusion of lymph nodes (OR, 0.031; 95%CI, 0.002-0.522). Fig. 2 shows the ROC curves for the prediction of EGFR mutations (the AUC for the full model was 0.898).

The final variables included lymph node size, lymph node status, emphysema, and lobulation. The power value of them was 0.99, 0.99, 0.99, and 0.99 respectively. Using the bonferroni method, the power value of the regression model was 0.97.

4. Discussion

This study demonstrated that emphysema, degree of primary tumor lobulation, and lymph node size and status were significantly associated with EGFR mutation status in cases of advanced pulmonary adenocarcinoma. Statistical analysis of these CT-features suggested they may be useful for predicting EGFR mutation status (the AUC of the ROC curve was 0.898). Prediction of EGFR mutations may be useful in deciding whether an invasive examination is suitable in some high-risk patients and whether repeat biopsy should be attempted in patients with discordant clinical features. Prediction of EGFR mutations may facilitate early planning and cost-effective treatments.

By univariate analysis, our study showed that EGFR mutations in advanced pulmonary adenocarcinomas were significantly associated

with females, non-smokers, and absence of emphysema; however, subsequent multivariate analysis only confirmed the significance of absence of emphysema. Previous studies showed that EGFR mutations are more frequent in tumors with adenocarcinoma histology, in non-smokers or light smokers, and in women with NSCLC [10,11,18,19]. However, other studies reported no association between the presence of EGFR mutations and sex or non-smoking status [12,20]. The differences between these studies may have been due to the heterogenous pathologic profiles of the patients leading to selection bias, different research parameters, and different statistical methods (e.g., some of these studies did not use multivariate analysis). Numerous studies have shown that smoking is associated with emphysema and that both are risk factors for lung cancer; additionally, emphysema as a lung cancer risk factor may not be entirely dependent on smoking [21–24]. Although squamous cell carcinoma is the most prevalent histopathological feature in emphysema- and smoking-related lung cancer, the presence of emphysema is also a risk factor for lung adenocarcinoma [23,24]. A large number of studies have investigated the correlation between smoking and EGFR mutations, but very few studies evaluated the correlation between emphysema and EGFR mutations [11]. Thus, further studies that examine correlations between smoking, emphysema, and EGFR-mutated NSCLC are needed.

Our study found a significant association between the degree of primary tumor lobulation and EGFR mutations status ($P < 0.001$). Shallow lobulation was present in 62.62% of EGFR + primary tumors but only in 21.28% of primary tumors with wild-type EGFR. Deep lobulation was present in 63.83% of tumors with wild-type EGFR but only in 29.91% of EGFR + tumors. Several studies attempted to describe the relationship between CT-features and EGFR mutation status. However, only a small portion of these previous studies included the evaluation of lobulation, and almost all of them reported no association between EGFR mutations and lobulation, which was simply described as presence or absence of lobulation [11–13]. In our study, only one patient lacked lobulation based on a presence/absence interpretation; thus, based on this qualitative assessment, there was no association between EGFR mutation status and lobulation, which is concordant with previous studies. However, when we graded lobulation (by defining the edge types of the “lobulated” class), EGFR + patients had significantly higher percentages of shallow lobulation and lower percentages of deep lobulation. To the best of our knowledge, no previous study used graded lobulation to evaluate the association between lobulation and EGFR mutations. Hasegawa et al. found a significant association between EGFR mutations and notch on multivariate analysis ($p = 0.0428$), although there was no statistically significant difference based on univariate analysis ($p = 0.9722$) (the “notch sign” is a particular form of lobulation defined as an abrupt bulging of the lesion contour) [10]. Some studies equated the notch with lobulation [25–27]; thus, our results are not comparable with these studies. Hsu et al. reported that an irregular shape of primary tumor was more common in adenocarcinomas with wild-type EGFR than in those with EGFR mutations [12]. We postulate that the irregular shape may be similar to or reflect the sign of deep lobulation.

It has been observed that cancer patients with EGFR gene mutations have longer survival times than those without EGFR gene mutations [28,29], which agrees with our results. The lobulation sign has the appearance of uneven arcs in the edge of tumors, which is attributable to different or uneven growth rates and is strongly associated with malignancy and invasiveness [30–32]. Relative to shallow lobulation, deep lobulation indicates greater malignancy and invasiveness and therefore reflects a worse prognosis.

Our study demonstrated that smaller lymph node size and lower percentages of partial fusion of lymph nodes were significantly associated with EGFR-mutation positive adenocarcinoma, based on both univariate and multivariate analyses. However, when lymph nodes were described as presence or absence of swollen lymph nodes, there was no association between EGFR mutations and lymph nodes. To the best of our knowledge, this finding has not been previously reported. However, Guan et al. reported that EGFR + patients had an earlier N stage than the group with wild-type EGFR based on PET/CT scans [33], which may be similar to our findings. This observation also reflects the lower malignancy and invasiveness of tumors in the EGFR + group as compared with the group with wild-type EGFR. The mechanism of this finding was uncertain and its value on clinical application needs to be further investigated.

Previous studies demonstrated that cancer patients with EGFR mutations, including NSCLC and thyroid carcinoma, often developed multiple pulmonary metastases, particularly miliary metastases [34–36]. Our study showed that EGFR mutations were associated with the presence of pulmonary and/or pleural metastatic nodules ($P = 0.006$) and with small metastatic nodule sizes ($P = 0.021$) based on univariate analysis, but subsequent multivariate analysis completely negated these associations. No significant associations between EGFR mutations and the distribution of metastatic nodules in lungs and pleura were observed in this study. Guan et al. reported that EGFR mutations in patients with NSCLC are associated with a higher incidence of distant brain and bone metastases but are not associated with distant liver and adrenals metastases [33]. In contrast to the study by Guan et al., our study showed no significant association between EGFR mutations and organs that are common sites of distant metastasis, such as bone, brain, adrenals, and liver. However, it is worth noting that the subjects in our study all had advanced pulmonary adenocarcinoma (stage IIIB, IIIC, or IV) whereas the Guan et al. study included patients with all stages of NSCLC (stage I-IV), which may account for the observed differences between our study and the Guan et al. study.

At present, there have been relatively few studies that evaluated potential correlations between pulmonary and pleura metastases, hilar and mediastinal lymph nodes, and organs associated with distant metastasis and EGFR mutations [33,34,37]. Further research on these relationships is needed, which may help to identify the similarities and differences between blood and lymphatic metastases and between wild-type EGFR and EGFR + NSCLC, which may help guide diagnosis and treatment.

In our study, none of the other primary tumor CT-features (location, lobe, size, density, calcifications, cavitation, vacuole sign, and air bronchogram) significantly associated with EGFR mutations based on multivariate analysis. Several published studies of the relationship between primary tumor size and EGFR mutations yielded inconsistent results; some studies demonstrated a significant association between EGFR mutations and smaller primary tumors [6,11,12,33,38], whereas other studies did not reach the same conclusion [13,19,39]. One study showed a significant correlation between EGFR mutations and larger tumors [40]. Currently, GGO is the most extensively studied CT-feature of tumor density, in terms of identifying correlations with EGFR mutations, but the results are controversial. Many retrospective studies have reported that GGO, a GGO ratio ≥50%, or higher GGO volume percentages were more frequent in tumors with EGFR mutations [6,7,38,41], but some studies revealed no significant associations between GGO and EGFR mutations [11,12]. Additionally, across these same studies, inconsistent calcifications, cavitation, and air bronchogram results were reported [9–13]. These differences may have been due to selection bias resulting from the heterogenous pathologic profiles of the patients, different patient stages, different research parameters, and different statistical methods.

In addition, the CT features of EGFR + pulmonary adenocarcinoma illustrated in this study can be exploited for pattern recognition by artificial intelligence (AI) systems that rely on big data and deep learning and also provide a basis for using AI systems to predict EGFR mutations based on CT images of advanced pulmonary adenocarcinoma. Although associations between CT-based radiomics or deep learning and mutations have been previously explored, most studies focused on early-stage or all stages of NSCLC and on primary tumors [14,42,43].This study demonstrated that emphysema, degree of

primary tumor lobulation, and lymph node size and status were significantly associated with EGFR mutation status in cases of advanced pulmonary adenocarcinoma. This suggests that when using deep learning or radiomics to predict EGFR mutation based on CT images of advanced pulmonary adenocarcinoma patients, we should not only focus on the primary tumor but also on lymph nodes and emphysema, which may improve the accuracy of diagnosis. At the same time, the significance of assessing the degree of primary tumor lobulation also puts forward higher requirements for the accurate detection and segmentation of images by an AI system. Huang et al. reported that interobserver variability of tumor contouring affects the use of radiomics for predicting EGFR mutation status [43], which was similar to our findings.

This study has several limitations. First, the retrospective design introduced selection bias that may have influence the final overall effect. Second, the sample size (n = 201) was relatively small; thus, the CT imaging features associated with EGFR mutations in advanced pulmonary adenocarcinoma need further confirmation with a subsequent larger study. Third, some of the CT features were evaluated only with qualitative procedures that may have lacked accuracy and repeatability. Finally, because not all CT examinations used a standard contrast enhancement protocol and only 72.41% of patients were examined by CT after enhancement, our analysis did not include CT features related to contrast enhancement of the lesions. The degree and type of enhancement is widely recognized as an important differential point in the differential diagnosis of lung cancer, but it is not clear whether it is related to EGFR mutations.

5. Conclusion

We found a significant correlation between CT imaging features (smaller lymph nodes, a lower percentage of deep lobulation of primary tumor and partial fusion of lymph nodes, and absence of emphysema) and EGFR mutations in advanced pulmonary adenocarcinoma. Evaluation of conventional CT features, including emphysema, degree of primary tumor lobulation, and lymph node size and status, helps to predict EGFR mutations status in advanced pulmonary adenocarcinoma. Moreover, these CT features suggest that the CT manifestations of the EGFR-mutation positive group were of lower malignancy and less invasive as compared to the wild-type EGFR group.

Disclosure

The authors declare no conflict of interest.

References

[1] L.A. Torre, F. Bray, R.L. Siegel, J. Ferlay, J. Lortet-Tieulent, A. Jemal, Global cancer statistics, 2012, CA Cancer J. Clin. 65 (2) (2015) 87–108.

[2] U. von Verschuer, R. Schnell, H.W. Tessen, J. Eggert, A. Binninger, L. Spring, M. Janicke, N. Marschner, T.L.K. Group, Treatment, outcome and quality of life of 1239 patients with advanced non-small cell lung cancer - final results from the prospective German TLK cohort study, Lung Cancer 112 (2017) 216–224.

[3] R. Buettner, J. Wolf, R.K. Thomas, Lessons learned from lung cancer genomics: the emerging concept of individualized diagnostics and treatment, J. Clin. Oncol. 31 (15) (2013) 1858–1865.

[4] S.E. Jorge, S.S. Kobayashi, D.B. Costa, Epidermal growth factor receptor (EGFR) mutations in lung cancer: preclinical and clinical data, Braz. J. Med. Biol. Res. 47 (11) (2014) 929–939.

[5] C.K. Lee, C. Brown, R.J. Gralla, V. Hirsh, S. Thongprasert, C.M. Tsai, E.H. Tan, J.C. Ho, T. Chu da, A. Zaatar, J.A. Osorio Sanchez, V.V. Vu, J.S. Au, A. Inoue, S.M. Lee, V. Gebski, J.C. Yang, Impact of EGFR inhibitor in non-small cell lung cancer on progression-free and overall survival: a meta-analysis, J. Natl. Cancer Inst. 105 (9) (2013) 595–605.

[6] M. Yano, H. Sasaki, Y. Kobayashi, H. Yukiue, H. Haneda, E. Suzuki, K. Endo, O. Kawano, M. Hara, Y. Fujii, Epidermal growth factor receptor gene mutation and computed tomographic findings in peripheral pulmonary adenocarcinoma, J. Thorac. Oncol. 1 (5) (2006) 413–416.

[7] Y. Yang, Y. Yang, X. Zhou, X. Song, M. Liu, W. He, H. Wang, C. Wu, K. Fei, G. Jiang, EGFR L858R mutation is associated with lung adenocarcinoma patients with dominant ground-glass opacity, Lung Cancer 87 (3) (2015) 272–277.

[8] K.H. Hsu, K.C. Chen, T.Y. Yang, Y.C. Yeh, T.Y. Chou, H.Y. Chen, C.R. Tsai, C.Y. Chen, C.P. Hsu, J.Y. Hsia, C.Y. Chuang, Y.H. Tsai, K.Y. Chen, M.S. Huang, W.C. Su, Y.M. Chen, C.A. Hsiung, G.C. Chang, C.J. Chen, P.C. Yang, Epidermal growth factor receptor mutation status in stage I lung adenocarcinoma with different image patterns, J. Thorac. Oncol. 6 (6) (2011) 1066–1072.

[9] C. Glynn, M.F. Zakowski, M.S. Ginsberg, Are there imaging characteristics associated with epidermal growth factor receptor and KRAS mutations in patients with adenocarcinoma of the lung with bronchioloalveolar features? J. Thorac. Oncol. 5 (3) (2010) 344–348.

[10] M. Hasegawa, F. Sakai, R. Ishikawa, F. Kimura, H. Ishida, K. Kobayashi, CT features of epidermal growth factor receptor-mutated adenocarcinoma of the lung: comparison with nonmutated adenocarcinoma, J. Thorac. Oncol. 11 (6) (2016) 819–826.

[11] S. Rizzo, F. Petrella, V. Buscarino, F. De Maria, S. Raimondi, M. Barberis, C. Fumagalli, G. Spitaleri, C. Rampinelli, F. De Marinis, L. Spaggiari, M. Bellomi, CT radiogenomic characterization of EGFR, K-RAS, and ALK mutations in non-small cell lung Cancer, Eur. Radiol. 26 (1) (2016) 32–42.

[12] J.S. Hsu, M.S. Huang, C.Y. Chen, G.C. Liu, T.C. Liu, I.W. Chong, S.H. Chou, C.J. Yang, Correlation between EGFR mutation status and computed tomography features in patients with advanced pulmonary adenocarcinoma, J. Thorac. Imaging 29 (6) (2014) 357–363.

[13] Z. Cheng, F. Shan, Y. Yang, Y. Shi, Z. Zhang, CT characteristics of non-small cell lung cancer with epidermal growth factor receptor mutation: a systematic review and meta-analysis, BMC Med. Imaging 17 (1) (2017) 5.

[14] Y. Liu, J. Kim, Y. Balagurunathan, Q. Li, A.L. Garcia, O. Stringfield, Z. Ye, R.J. Gillies, Radiomic features are associated with EGFR mutation status in lung adenocarcinomas, Clin. Lung Cancer 17 (5) (2016) 441–448 e6.

[15] H. Wang, M.B. Schabath, Y. Liu, Y. Han, Q. Li, R.J. Gillies, Z. Ye, Clinical and CT characteristics of surgically resected lung adenocarcinomas harboring ALK rearrangements or EGFR mutations, Eur. J. Radiol. 85 (11) (2016) 1934–1940.

[16] E.Y. Kim, E.N. Cho, H.S. Park, A. Kim, J.Y. Hong, S. Lim, J.P. Youn, S.Y. Hwang, Y.S. Chang, Genetic heterogeneity of actionable genes between primary and metastatic tumor in lung adenocarcinoma, BMC Cancer 16 (2016) 27.

[17] K. Taniguchi, J. Okami, K. Kodama, M. Higashiyama, K. Kato, Intratumor heterogeneity of epidermal growth factor receptor mutations in lung cancer and its correlation to the response to gefitinib, Cancer Sci. 99 (5) (2008) 929–935.

[18] H. Shigematsu, L. Lin, T. Takahashi, M. Nomura, M. Suzuki, I.I. Wistuba, K.M. Fong, H. Lee, S. Toyooka, N. Shimizu, T. Fujisawa, Z. Feng, J.A. Roth, J. Herz, J.D. Minna, A.F. Gazdar, Clinical and biological features associated with epidermal growth factor receptor gene mutations in lung cancers, J. Natl. Cancer Inst. 97 (5) (2005) 339–346.

[19] M. Sugano, K. Shimizu, T. Nakano, S. Kakegawa, Y. Miyamae, K. Kaira, T. Araki, M. Kamiyoshihara, O. Kawashima, I. Takeyoshi, Correlation between computed tomography findings and epidermal growth factor receptor and KRAS gene mutations in patients with pulmonary adenocarcinoma, Oncol. Rep. 26 (5) (2011) 1205–1211.

[20] T.W. Jang, C.H. Oak, H.K. Chang, S.J. Suo, M.H. Jung, EGFR and KRAS mutations in patients with adenocarcinoma of the lung, Korean J. Intern. Med. 24 (1) (2009) 48–54.

[21] M. Bellomi, C. Rampinelli, G. Veronesi, S. Harari, F. Lanfranchi, S. Raimondi, P. Maisonneuve, Evolution of emphysema in relation to smoking, Eur. Radiol. 20 (2) (2010) 286–292.

[22] B.A. Forey, A.J. Thornton, P.N. Lee, Systematic review with meta-analysis of the epidemiological evidence relating smoking to COPD, chronic bronchitis and emphysema, BMC Pulm. Med. 11 (2011) 36.

[23] Y. Li, S.J. Swensen, L.G. Karabekmez, R.S. Marks, S.M. Stoddard, R. Jiang, J.B. Worra, F. Zhang, D.E. Midthun, M. de Andrade, Y. Song, P. Yang, Effect of emphysema on lung cancer risk in smokers: a computed tomography-based assessment, Cancer Prevent. Res. (Philadelphia, Pa.) 4 (1) (2011) 43–50.

[24] P.N. Lee, B.A. Forey, K.J. Coombs, Systematic review with meta-analysis of the epidemiological evidence in the 1900s relating smoking to lung cancer, BMC Cancer 12 (2012) 385.

[25] A. Snoeckx, P. Reyntiens, D. Desbuquoit, M.J. Spinhoven, P.E. Van Schil, J.P. van Meerbeeck, P.M. Parizel, Evaluation of the solitary pulmonary nodule: size matters, but do not ignore the power of morphology, Insights Imaging 9 (1) (2018) 73–86.

[26] C.V. Zwirewich, S. Vedal, R.R. Miller, N.L. Muller, Solitary pulmonary nodule: high-resolution CT and radiologic-pathologic correlation, Radiology 179 (2) (1991) 469–476.

[27] K. Kuriyama, R. Tateishi, O. Doi, K. Kodama, M. Tatsuta, M. Matsuda, T. Mitani, Y. Narumi, M. Fujita, CT-pathologic correlation in small peripheral lung cancers, AJR Am. J. Roentgenol. 149 (6) (1987) 1139–1143.

[28] R. Nakamura, Y. Inage, R. Tobita, K. Mori, T. Numata, H. Yanai, T. Endo, H. Ohtani, H. Satoh, K. Yuzawa, M. Koizumi, H. Ueki, Epidermal growth factor receptor mutations: effect on volume doubling time of non-small-cell lung cancer patients, J. Thorac. Oncol. 9 (9) (2014) 1340–1344.

[29] T. Kosaka, Y. Yatabe, R. Onozato, H. Kuwano, T. Mitsudomi, Prognostic implication of EGFR, KRAS, and TP53 gene mutations in a large cohort of Japanese patients with surgically treated lung adenocarcinoma, J. Thorac. 4 (1) (2009) 22–29.

[30] H.J. Lee, J.M. Goo, C.H. Lee, C.M. Park, K.G. Kim, E.A. Park, H.Y. Lee, Predictive CT findings of malignancy in ground-glass nodules on thin-section chest CT: the effects on radiologist performance, Eur. Radiol. 19 (3) (2009) 552–560.

[31] S.M. Lee, C.M. Park, J.M. Goo, H.J. Lee, J.Y. Wi, C.H. Kang, Invasive pulmonary adenocarcinomas versus preinvasive lesions appearing as ground-glass nodules: differentiation by using CT features, Radiology 268 (1) (2013) 265–273.

[32] G.A. Soardi, S. Perandini, M. Motton, S. Montemezzi, Assessing probability of malignancy in solid solitary pulmonary nodules with a new Bayesian calculator:

improving diagnostic accuracy by means of expanded and updated features, Eur. Radiol. 25 (1) (2015) 155–162.
[33] J. Guan, M. Chen, N. Xiao, L. Li, Y. Zhang, Q. Li, M. Yang, L. Liu, L. Chen, EGFR mutations are associated with higher incidence of distant metastases and smaller tumor size in patients with non-small-cell lung cancer based on PET/CT scan, Med. Oncol. 33 (1) (2016) 1.
[34] Y. Togashi, K. Masago, T. Kubo, Y. Sakamori, Y.H. Kim, Y. Hatachi, A. Fukuhara, T. Mio, K. Togashi, M. Mishima, Association of diffuse, random pulmonary metastases, including miliary metastases, with epidermal growth factor receptor mutations in lung adenocarcinoma, Cancer 117 (4) (2011) 819–825.
[35] K. Park, K. Goto, A review of the benefit-risk profile of gefitinib in Asian patients with advanced non-small-cell lung cancer, Curr. Med. Res. Opin. 22 (3) (2006) 561–573.
[36] K. Masago, R. Asato, S. Fujita, S. Hirano, Y. Tamura, T. Kanda, T. Mio, N. Katakami, M. Mishima, J. Ito, Epidermal growth factor receptor gene mutations in papillary thyroid carcinoma, Int. J. Cancer 124 (11) (2009) 2744–2749.
[37] D.Y. Shin, I.I. Na, C.H. Kim, S. Park, H. Baek, S.H. Yang, EGFR mutation and brain metastasis in pulmonary adenocarcinomas, J. Thorac. Oncol. 9 (2) (2014) 195–199.
[38] K. Usuda, M. Sagawa, N. Motono, M. Ueno, M. Tanaka, Y. Machida, M. Matoba, M. Taniguchi, H. Tonami, Y. Ueda, T. Sakuma, Relationships between EGFR mutation status of lung cancer and preoperative factors - are they predictive? Asian Pac. J. Cancer Prev. 15 (2) (2014) 657–662.
[39] M.H. van Gool, T.S. Aukema, E.E. Schaake, H. Rijna, H.E. Codrington, R.A. Valdes Olmos, H.J. Teertstra, R. van Pel, S.A. Burgers, H. van Tinteren, H.M. Klomp, (18)F-fluorodeoxyglucose positron emission tomography versus computed tomography in predicting histopathological response to epidermal growth factor receptor-tyrosine kinase inhibitor treatment in resectable non-small cell lung cancer, Ann. Surg. Oncol. 21 (9) (2014) 2831–2837.
[40] K.H. Ko, H.H. Hsu, T.W. Huang, H.W. Gao, D.H. Shen, W.C. Chang, Y.C. Hsu, T.H. Chang, C.M. Chu, C.L. Ho, H. Chang, Value of (1)(8)F-FDG uptake on PET/CT and CEA level to predict epidermal growth factor receptor mutations in pulmonary adenocarcinoma, Eur. J. Nucl. Med. Mol. Imaging 41 (10) (2014) 1889–1897.
[41] H.J. Lee, Y.T. Kim, C.H. Kang, B. Zhao, Y. Tan, L.H. Schwartz, T. Persigehl, Y.K. Jeon, D.H. Chung, Epidermal growth factor receptor mutation in lung adenocarcinomas: relationship with CT characteristics and histologic subtypes, Radiology 268 (1) (2013) 254–264.
[42] E. Rios Velazquez, C. Parmar, Y. Liu, T.P. Coroller, G. Cruz, O. Stringfield, Z. Ye, M. Makrigiorgos, F. Fennessy, R.H. Mak, R. Gillies, J. Quackenbush, H. Aerts, Somatic mutations drive distinct imaging phenotypes in lung cancer, Cancer Res. 77 (14) (2017) 3922–3930.
[43] Q. Huang, L. Lu, L. Dercle, P. Lichtenstein, Y. Li, Q. Yin, M. Zong, L. Schwartz, B. Zhao, Interobserver variability in tumor contouring affects the use of radiomics to predict mutational status, J. Med. Imaging (Bellingham, Wash.) 5 (1) (2018) 011005.